DUAL-OBJECTIVES BASED OPTIMIZATION OF ORGANIC RANKINE CYCLE USING GENETIC ALGORITHM

***Muhammad Tahir Ameen, Nasir Hayat, Haris Hussain,**
Muhammad Asif Mahmood Qureshi, Asad Raza Gardezi
Faculty of Mechanical Engineering, University of Engineering and Technology, Lahore 54890 – Pakistan
*Corresponding Author: tahir.ameen@uet.edu.pk

***ABSTRACT**: Organic Rankine Cycle with various organic compounds is increasingly being used for low potential waste heat recovery systems. In order to further promote their use thermal efficiency should be maximized and specific investment cost need to be minimized at the same time. In this work several organic compounds (R-123, R-1234ze, R-152a, R-21, R-236ea, R-245ca and R-601) have been employed to evaluate the thermo-economic performance of Organic Rankine Cycle system. Thermodynamic and economic models have been generated with the help of MATLAB version R2012a and dual-criteria optimization has been carried out using non-dominated sorting genetic algorithm (II) method. The results show that R-21 outperforms in terms of thermodynamic behavior whereas R-245ca is best from specific investment cost viewpoint.*

Keywords: Organic Rankine Cycle, Genetic Algorithm, Dual-objective optimization, Thermal efficiency, Specific Investment Cost, Waste Heat Recovery, Plate type heat exchanger

1. INTRODUCTION

Because of increased prices of non-renewable fuel energy it is becoming really difficult for the world to tackle the situation. Energy crisis need prime attention to be managed in modern era. Apart from being uneconomical there is another major issue which is pollution caused by hydrocarbons fuel energy being used on large scale in industrial plants and transportation. Global warming and ozone depletion has asked the researchers to find out new ways for such techniques which are risk free in terms of pollution and also involve full utilization of any sort of waste energy to reduce unnecessary entry of waste energy into atmosphere. So coping with energy deficiency and reduction of environmental pollution are two big challenges. In this scenario it is demanded that such resources of energy which are not only cheap but also environmental friendly should be utilized. Therefore different renewable energy resources are being explored, technically implemented and improved day by day to meet the needs.

One such technique is exploiting the low potential waste heat originating from different industrial plants or geothermal sources which would otherwise be wasted. Such heat is of low grade and is discharged into the atmosphere. The industrial plants eject large amount of heat in the form of warm liquids and gaseous effluents straight into the atmosphere because of scarcity of efficient techniques for recovery and utilization. One solution of WHR is using ORC system [1-3]. This technique will not only provide additional source of electricity but also cause to reduce green-house gas emissions and global warming. ORC system involves an organic compound as working substance instead of water which is a working substance for conventional cycles.

Different researchers have been investigating for past two decades different organic systems and involved equipment running under different operating parameters. Most of the researchers focused on investigating variety of performance indicators of the system [4-8] whereas few considered economics of ORC system [9]. As a whole attention was paid to integrate ORC systems with Waste Heat Recovery applications and find out the best type of working fluid suitable for particular application. Intention was clearly to optimize ORC system for better working under limited resources. Furthermore it is found after going through literature that multi-objective optimization can be used effectively to find optimal solutions for those objectives which afflict with each other such as thermo-economic optimizations [10-14].

Yamamoto T. et al. [1] covered the importance of ORC system as low grade heat source application. Optimum operating conditions were estimated using R-123 employing a numerical simulation model. Desai N. B. et al. [2] focused on advantages of ORC over conventional Rankine cycle. Thermal efficiency can be improved by varying the architectures of ORCs. The benefits of integrating the ORC system with waste heat recovery background process have been illustrated using examples. The study done by Carcasci C. et al. [15] illustrates the results of the simulations of an ORC combined with gas turbine for obtaining electrical energy. Best choice was made by the comparison of four working fluids and it was concluded that different working fluids are best under different conditions. A. Rettig1, M. Lagler et al. [16] estimated the potential of new ORC applications. The research shows a brief introduction of ORC system followed by statistical evaluation of existing ORC applications. Depending on the industrial process the waste energy is rejected at different temperatures, which makes the optimal choice of the working fluid of great importance. Therefore a few aspects of the working fluid selection procedure are presented and the economical attractiveness of ORC systems is assessed. Bao J. et al. [4] reviewed how to select the working fluids along with expanders in ORC systems. The analysis included the influence of working fluids type as well as the thermo-physical properties on system. Much work has been done in regard of how to choose the organic compounds as working fluids for implementing in ORC systems [5-8, 17]. Bruno J.C. et al. [17] modeled and optimized solar ORC engines for reverse osmosis desalination for remote areas. A selection of working fluid candidates was made and after doing two case studies it was concurred that studied system was better than equivalent photovoltaic system. J.P. Roy et al. [18] analyzed regenerative ORC system based upon parametric optimization implementing R-123 and R-134a in the system. They aimed at getting a better working fluid on the basis of a variety of performance indicators. They found that R-123 had upper hand over R-134a. Maraver D. et al. [19] focused on thermodynamic optimization of ORC for power and CHP (combined heating and power) from different average heat source profiles. Their goal was to provide guidelines for a wide range of operating conditions, for subcritical and transcritical, regenerative and non-regenerative cycles. They assessed the main equipment in

the cycle and proposed an optimized model to predict best cycle performance in terms of efficiency with different working fluids. Quoilin S. et al. [20] presented the overview of different ORC applications. In the study a market review is proposed that includes cost analysis of different ORC systems. Technological constraint parameters and optimization methods were described in detail and discussed. Wang D. et al. [21] proposed a double ORC system for discontinuous WHR. In the research the optimal running conditions have been evaluated for various working fluids by using algorithm approach in MATLAB. The influence of exit temperature of the heat source on various performance indicators such as thermal efficiency, power, flow rate, irreversibility and exergy have been analyzed.

Xi H. et al. [22] examined the performances of three different ORC architectures including the basic ORC, single stage ORC and double stage ORC using six different working fluids under same waste heat conditions. They set exergy efficiency as objective function and chose GA to determine the optimal fractions of the flow rates. Their results show that for each working fluid, the double stage system gave best efficiency under optimal operating conditions followed by single stage system and the basic ORC system had the worst efficiencies. R-11 and R-141b were recommended because of their superior thermodynamic properties.

Imran M. et al. [10] carried out thermo-economic optimization of basic as well as regenerative ORC systems by using NSGA-II with respect to two objective functions including five different refrigerants. The research came up with R-245fa to be the best under provided conditions. In another study Imran M. et al. [11] worked on economic design of evaporator for an ORC system keeping minimum pressure drop and minimum cost as objective functions and geometrical parameters were the decision variables. He presented optimal values after detailed analysis. Wang J. et al. conducted thorough investigation over ORC system [12-14]. He performed multi-objective optimization of system using R-134a as working medium to obtain system optimal design from thermo-economic point of view using NSGA-II method. Maximization of exergy efficiency and minimization of overall cost of system were declared as objective functions. The results pointed out that increase in exergy efficiency gives rise to total cost of the system. He concurred that the optimal value for exergy efficiency is 13.98% and that for system cost is 129.28×10^4 USD [12]. In other research he examined the effect of key design parameters on net power output and heat transfer surface areas of evaporator and condenser using R-123, R-245fa and isobutane. System was optimized keeping net power output to heat transfer area as evaluating criterion using genetic algorithm. Isobutane proved to be the best [13]. In a further study condenser design was modelled using PHE and effect of geometrical parameters on heat transfer area and pressure drop was investigated. NSGA-II was employed as optimization method to find optimal solution for minimum heat transfer area and pressure drop and conclusion was that decrease in total heat transfer area can increase the pressure drop [14].

J.R. Garcı´a-Cascales et al. [23] studied PHEs used as evaporators and condensers. The author investigated representative variables which are evaporation and condensing temperatures and compared several heat transfer coefficients using R-22 and R-290 and showed that results correspond to those done in earlier studies. Zahid H. Ayub [24] presented a literature review on PHEs. He introduced new correlations for evaporation heat transfer coefficient along with friction factor. Besides this evaporation and condensation heat transfer and corresponding friction factor correlations have been worked on using R-410A and R-22 with different geometric configurations of PHEs [25-27].

Survey of available literature reveals that specifically plate type of heat exchangers which are integral part of ORC systems need be focused so as to adjust their thermodynamic, hydraulic and economic performances. GA has proved to be a great evolutionary algorithm that can tackle easily the optimization for the systems that primarily involve conflicting, non-linear and complex objective functions. Furthermore as far as working medium is concerned a refrigerant which is best in specific operating conditions may be worse in other operating conditions [15]. So there are various challenges including how efficiently ORC system can be used with minimum amount of cost required for a complete system to run with intended results. Therefore an effort has been made here to design an ORC system, decide objective functions and influencing decision variables, scrutinize the refrigerants out of large number of available refrigerants [4] and check their performance individually using genetic algorithm within MATLAB. Multi-objective optimization has not been given much utilization in investigating such thermal energy systems. The selected refrigerants specifically R-245ca have not been compared with each other on their performance basis in the past. The ORC system has been optimized here thermo-economically by using wide range application of the decision variables (Section 8.1).

2. METHODOLOGY

After selection of a set of suitable refrigerants as working media for ORC system, in the current study two objective functions were selected which are thermal efficiency of system and corresponding specific investment cost. The theme is to increase the thermal efficiency and reduce the specific investment cost of the system operating under considered conditions. The four influencing decision variables are evaporation pressure, superheat, PPTD across evaporator and condenser. These parameters have strong effect on the objective functions set. Process was mathematically modeled. Thermodynamic and economic models were developed and written in MATLAB in a function format. The multi-objective global optimization tool was used so as to evaluate the dual-objectives function. Constraints and bounds were applied for the decision variables in accordance with considered conditions. Iterative procedure based upon secant method was used within the function format in order to design the heat exchangers of the system. Function evaluation involves this iterative process each time to define the heat exchanger sizing for selected decision variable values. Within each function evaluation, iterative process continues until there is no further change in objective function values between consecutive generations. The working fluid thermodynamic and transport properties were calculated by calling REFPROP version 9.0 given by NIST using subroutines in the MATLAB. After obtaining results sensitivity analysis was done on three refrigerants.

3. WORKING FLUIDS SELECTION

Safety, environmental, material, thermodynamic performance and economics of ORC systems are the aspects that need to be taken into account for the selection of working fluids in a system. In past, many researchers have investigated various organic compounds by implementing them in a system with the objective of

optimization of different performance indicators of the system [10-14, 18, 21, 22]. Different performance indicators and different running and simulating conditions showed different organic compounds being best as working fluids. There is a lot of research space in this part of optimization of the ORC system. By the time many organic compounds are being phased out because of their inability to match with the demanding environmental properties. Focus must be on such compounds which give suitably best performance in thermodynamic systems, are safe to use and healthy for environment. Because of variety of temperature ranges available for ORC systems, various working conditions and hundreds of available organic compounds the task of choosing the best organic compound as a working fluid seems quite hectic but worth investigating. A few key points are discussed here which help in preliminary selection of compounds.

It is suggested that as a whole the working fluid category (dry, isentropic or wet) and thermo-physical properties should be used as initiatives to select the working fluid for particular application [4]. When wet fluids are used it is demanded that a superheater should be there to superheat the saturated vapors before turbine inlet so as to keep the turbine blades out of the trouble of being eroded towards exit [5]. A minimum of 85% of dryness fraction is recommended at the turbine exit [4, 5]. Moreover because of installation of extra component i.e. superheater the SIC rises. For isentropic fluids the vapors remain saturated throughout the expansion process and there is no need for superheating or regenerating. This makes isentropic fluids the most ideal working fluids [9]. Like isentropic fluids dry fluids don't require superheating. Isentropic and dry fluids are the most favorable working fluids [2, 4, 7]. If the fluid is too dry, regeneration is done to gain the maximum potential out of superheated vapors which however increases SIC.

With respect to thermo-physical properties it is seen that suitably smaller latent heat of vaporizations of working fluids effects positively on the gross performance. High vapor density is a key as lower vapor density results in larger volume flow rate which in turn causes higher pressure drops in the heat exchangers and larger sized turbine is then demanded [8]. Specific heat of working fluid has no obvious relationship with the power output [4]. Higher critical temperatures for working fluids result in higher first law thermal efficiencies but lower condensing pressure [17] and fluids with higher critical temperatures should be used only for high temperature WHR sources [8]. Freezing point should be below the smallest temperature at any point in the ORC so as to prevent any solidification. Turbine efficiency increases with using higher molecular weight organic compounds but it requires oversizing of heat exchanger [6]. Such organic compounds should be selected that have lower viscosity in liquid and vapor phases so that the tendency to cause pressure drops in heat exchanger is eliminated and higher heat transfer coefficient can be achieved by using compounds with higher thermal conductivity [4].

Global Warming Potential and Ozone Depletion Potential are the parameters that concern a great deal. These are the numerical measures of the potential towards ozone depletion and producing global warming. Both are required to be minimal. Safety requires that working fluids be non-toxic and non-flammable [3, 6].

The discussion end is that not a single working fluid can be taken as the best for ORC system. A few refrigerants may be thermodynamically very good but may be risky to use as far as environmental aspects and considerations are concerned. Keeping the above mentioned parameters in mind, temperature levels of heat source and cooling medium and having a throughout study of published articles dealing with ORC systems, for the current study seven organic compounds are selected. The thermo-physical properties are enlisted in the Table 1

4. SYSTEM CONFIGURATION

An ORC system consists of five major components. The schematic shows four major components of the system Fig. 1. Fifth component is the working substance.

The thermodynamic cycle for ORC system consists of four processes

1. Process 1-2: Heat addition at constant pressure in evaporator
2. Process 2-3: Isentropic expansion in the turbine
3. Process 3-4: Heat rejection in condenser at constant pressure
4. Process 4-1: Isentropic compression in circulation

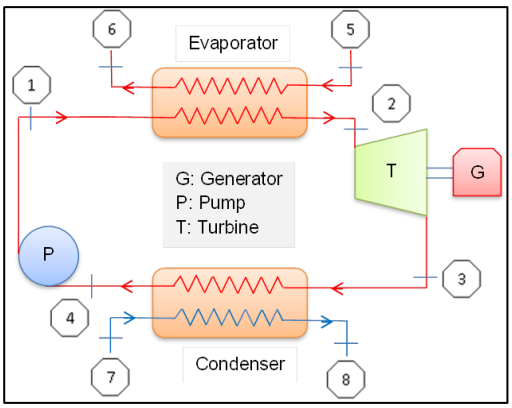

Fig. 1 The Schematic of ORC

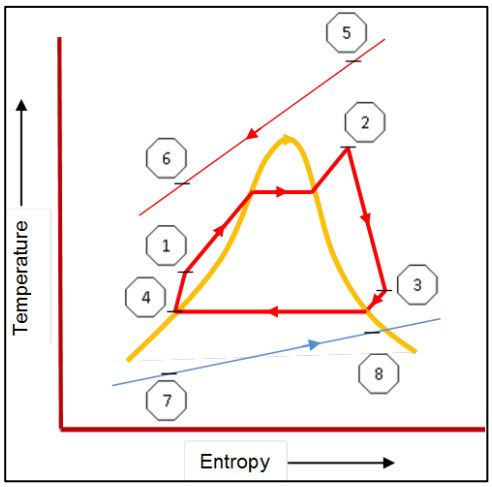

Fig. 2 The T-s Diagram of ORC

Pump.

In the evaporator (Process 1-2) the heat carrier source delivers its heat to the working fluid and as a result the working fluid is vaporized from its liquid state thus raising its temperature to turbine inlet temperature, the process ideally being taken place at constant pressure. The process can be split into two sections if there is no superheating or three sections if there is superheating. Very first section is preheating section where the working fluid temperature is raised from its pump exit temperature to vaporization temperature. Phase change takes place in vaporization section by absorption of latent heat. After all liquid transforms into vapors superheating is required at times to enhance the temperature of the working fluid beyond its

Table 1 Organic working fluids employed in ORC system

Type	ASHRAE Number	ODP	GWP	Molecular Mass (kg/kmol)	Boiling Point (◦C)	Critical Temperature (◦C)	Critical Pressure (kPa)	Fluid Type	Safety Group*
HCFC	R-123	0.012	120	152.93	27.85	183.79	3674	Dry	B1
HFO	R-1234ze	0	6	114.04	−19.0	109.36	3636	Isentropic	A2L
HFC	R-152a	0	124	66.06	−24.03	113.26	4517	Wet	A2
HCFC	R-21	0.04	151	102.92	8.86	178.33	5181	Wet	B1
HFC	R-236ea	0	1370	152.04	6.18	139.29	3502	Dry	A2
HFC	R-245ca	0	693	134.05	25.13	174.42	3925	Dry	n/a
HC	R-601	0	5	72.15	36.06	196.56	3370	Dry	A3

* ASHRAE Standard 34 - Refrigerant safety group classification; n/a: not available

1: No flame propagation; 2: Lower flammability; 3: Higher flammability; A: Lower toxicity; B: Higher toxicity; 2L: Lower flammability and maximum burning velocity of less than 10 cm/s; N/A: not available

vaporization temperature in order to make sure that during expansion in turbine there is lesser percentage of moistures left to damage the turbine blades and change the metallurgical properties of its material [4, 5]. Expansion of high temperature and pressure vapors in turbine (Process 2-3) occurs hence causes the turbine to gain useful kinetic energy. After expansion there is vapor condenser which is meant for bringing the working fluid to its liquid state (Process 3-4) for pump action to begin. Desuperheating and condensation are two stages gone through by the condensing vapors. Desuperheating brings the superheated vapors down to meet the saturated vapor line where condensation starts by the extraction of the latent heat of condensation from theworking fluid via a secondary fluid on the opposite side of heat exchanger. It is assumed that there is no subcooling for the current study. So pump takes the working fluid essentially in saturated liquid state and raises its pressure to evaporation pressure (Process 4-1). The cycle thus continues. Fig. 2 describes the T-S diagram of the cycle. Process: 5-6 demostrates heat source and Process: 7-8 depicts state change of cooling medium.

5. PROCESS MODELING

The heat obtained by the organic working fluid in evaporator is given as

$$Q_{evap} = \dot{m}_r \left(h_2 - h_1\right) \quad (1)$$

The turbine work extracted during expansion is

$$W_{turb} = \dot{m}_r \eta_{turb} \left(h_2 - h_3\right) \quad (2)$$

Heat denied by the working fluid in the vapor condenser is

$$Q_{cond} = \dot{m}_r \left(h_3 - h_4\right) \quad (3)$$

Pump work consumption is

$$W_{pump} = \frac{\dot{m}_r \left(h_1 - h_4\right)}{\eta_{pump}} \quad (4)$$

The thermal efficiency of Organic Rankine Cycle is

$$\eta_{th} = \frac{\left(W_{turb} - W_{pump}\right)}{Q_{evap}} \quad (5)$$

6. HEAT EXCHANGRS DESIGN

The rotary equipment i.e. turbine and pump have not been investigated in the ongoing study in detail and the design of the system is limited to designing the two heat exchangers separately required for meeting the particular heat duty requirements kept under certain value of allowable pressure drop (5% of inlet). Turbine and pump are designed based upon their thermodynamic efficiencies of 0.75 and 0.65 correspondingly [10]. Evaporator and condenser heat exchangers chosen are chevron type plate heat exchangers selected because of their better performance over shell and tube type [28]. Both heat exchangers are modelled on the basis of LMTD method having counter current flow condition. Stainless steel AISI-304 is the material for two chevron type heat exchangers [29]. Design of heat exchangers requires iterative procedure to be followed in order to determine the true value of number of thermal plates which satisfies the heat transfer surface area demanded by the energy balance. The calculations need to start by considering specific geometry of heat exchanger prematurely. The geometry selected for PHEs is described in tabular form in Table 2. As mentioned above the number of thermal plates, Np works as the variable element to be found by iterative procedure. The design layout of heat exchangers is shown in the Fig. 4.

Few assumptions are taken into account in regard of working with PHE which involve having steady state conditions, fully developed flow in channels, negligible heat lose to surroundings and minimum fouling effects [13].

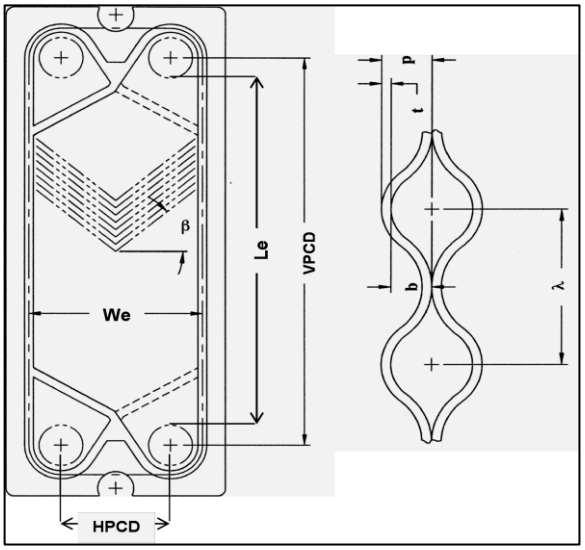

Fig. 3 Basic geometry of Plate Heat Exchanger [24]

6.1. Geometry Considerations

The geometry of PHE is of utmost importance and carries a lot of considerations in designing. The most common parameters include plate thickness, plate pitch, mean channel spacing, enlargement factor, chevron angle, hydraulic and equivalent diameters, corrugation pitch and port diameters. These are shown in Table 2 along with considered values. The geometry is illustrated in the Fig. 3. For the sake of briefness above mentioned parameters have not been defined in detail here as they are found in literature [23-27, 29].

Based upon overall dimensions the total area of PHE is related as

$$A_{total} = \left(N_p - 2\right) A_p \quad (6)$$

Here $A_p = L_e W_e$ is the area of a single plate.

Hydraulic and equivalent diameters are

$$D_h \cong \frac{2b}{\Phi} when b \square W_e \quad (7)$$

$$D_e \cong 2b \quad (8)$$

6.2. Thermodynamic Modeling

The evaporator and condenser heat exchangers both include heat transfer in single-phase as well as two-phase. There are three sections for evaporator PHE and two sections for condenser PHE. Each section or zone has its own number of thermal plates, heat transfer area and heat transfer coefficient. The three sections defined in evaporator PHE are preheating (I), vaporization (II) and superheating (III). The total area of evaporator is

$$A_{evap} = A_{sp,I} + A_{tp,II} + A_{sp,III} \quad (9)$$

During preheating single phase heat transfer occurs as both sides fluids are in liquid phase. Vaporization deals with two-phase heat transfer as the working fluid is in mixed phase i.e. partly liquid and partly vapors. Superheating has single- phase heat transfer working fluid being totally in superheated vapor state.

The vapor condenser PHE has two sections which are desuperheating (IV) and condensing (V). The desuperheating section participates in single phase heat transfer while condensing section in two-phase because the working fluid is in mixed phase. The total area of vapor condenser PHE is governed as

$$A_{cond} = A_{sp,IV} + A_{tp,V} \quad (10)$$

Heat transfer in single phase

Single phase sections are preheater (1), superheater (III) and desuperheater (IV). It is observed that when algorithm chooses those values of decision variables that include superheat as zero, the superheating section does no longer exist. Similarly if the turbine exit gives mixed state of working substance rather than superheated state, the desuperheating section does not exist.

Heat transfer in single phase section is given below

$$Q_{sp} = U_{sp} A_{sp} LMTD_{sp} \quad (11)$$

Log mean temperature difference is

$$LMTD_{sp} = \frac{\Delta T_{\max} - \Delta T_{\min}}{\log\left(\frac{\Delta T_{\max}}{\Delta T_{\min}}\right)} \quad (12)$$

The overall heat transfer coefficient of single phase section is

$$\frac{1}{U_{sp}} = \frac{1}{\alpha_w} + \frac{t_p}{k_p} + \frac{1}{\alpha_{r,sp}} \quad (13)$$

The Nusselt No. correlation [23] for single phase water side heat source is

$$Nu_w = 0.724\left(\frac{6\beta}{\pi}\right)^{0.646} \mathrm{Re}^{0.583}\,\mathrm{Pr}^{0.33} \quad (14)$$

The Reynolds No. Re is given by

$$\mathrm{Re} = \frac{GD_h}{\eta} \quad (15)$$

Here G is channel mass flux presented as

$$G = \frac{\dot{m}}{N_{ch} b W_e} \quad (16)$$

The Prandtl No. is Pr given by

$$\mathrm{Pr} = \frac{C_p \eta}{\lambda} \quad (17)$$

The convective heat transfer coefficient is given as

$$\alpha_w = \frac{Nu_w k_w}{D_h} \quad (18)$$

The Nusselt No. correlation [25] for single phase refrigerant in a plate type of heat exchanger is given

$$Nu_{r,sp} = 0.2092\,\mathrm{Re}^{0.78}\,\mathrm{Pr}^{0.33}\left(\frac{\mu_m}{\mu_{wall}}\right)^{0.14} \quad (19)$$

The convective heat transfer coefficient is then given

$$\alpha_{r,sp} = \frac{Nu_{r,sp} k_r}{D_h} \quad (20)$$

Table 2 Dimensional parameters of PHEs

Designation (Units)	Design values	
	Evaporator	Condenser
VPCD (m)	1.45	1.5
HPCD (m)	0.35	0.3
W_e (m)	0.55	0.55
L_e (m)	1.25	1.25
p (m)	0.0035	0.0045
t (m)	0.0005	0.0005
b (m)	0.003	0.004
A_f (m^2)	0.00165	0.0022
λ (m)	0.01	0.013
A_{ip} (m^2)	0.6875	0.6875
φ	1.1968	1.1968
A_p (m^2)	0.8228	0.8228
D_h (m)	0.005	0.0067
D_e (m)	0.006	0.008
β (°)	60	60

Pressure drop in single phase

There is only one component of pressure drop i.e. frictional pressure drop for both heat source and heat sink sides in case of single phase heat transfer. Other pressure drop components are neglected for the ongoing study. It is described as

$$\Delta P_f = \frac{4 f_{sp} N_{ch} G^2 L_e}{2\rho D_h} \quad (21)$$

The frictional pressure drop for both heat source and heat sink sides is correlated as [24]

$$f_{sp} = \frac{0.572}{\mathrm{Re}^{0.217}} \; for \; \mathrm{Re} > 550 \quad (22)$$

Heat transfer in two phase

There are two two-phase sections encountered during heat transfer in the system which are evaporation (II) and condensation (V).

Heat transfer in any two phase section is given below

$$Q_{tp} = U_{tp} A_{tp} LMTD_{tp} \quad (23)$$

The Log Mean Temperature Difference is as follows

$$LMTD_{tp} = \frac{\Delta T_{\max} - \Delta T_{\min}}{\log\left(\frac{\Delta T_{\max}}{\Delta T_{\min}}\right)} \quad (24)$$

The overall heat transfer coefficient in two-phase is

$$\frac{1}{U_{tp}} = \frac{1}{\alpha_w} + \frac{t_p}{k_p} + \frac{1}{\alpha_{r,tp}} \quad (25)$$

For both evaporation and condensation sections the Nusselt No. and corresponding heat transfer coefficient for heat source and cooling water sides are used as expressed in eqns.14 and 18. For refrigerant the Nusselt No. correlation [26] during evaporation in a vertical PHE as given as

$$Nu_{r,tp,II} = Ge_1 \,\mathrm{Re}_{eq}^{Ge_2}\, Bo_{eq}^{0.3}\,\mathrm{Pr}^{0.4} \quad (26)$$

$$Ge_1 = 2.81\left(\frac{P_{co}}{D_h}\right)^{-0.041}\left(\frac{\pi}{2}-\beta\right)^{-2.83} \quad (27)$$

$$Ge_2 = 0.746\left(\frac{P_{co}}{D_h}\right)^{-0.082}\left(\frac{\pi}{2}-\beta\right)^{0.61} \quad (28)$$

$$\mathrm{Re}_{eq} = \frac{G_{eq} D_h}{\mu_f} \quad (29)$$

$$G_{eq} = G\left[(1-x)+x\left(\frac{\rho_f}{\rho_g}\right)^{0.5}\right] \quad (30)$$

$$Bo_{eq} = \frac{q''}{G_{eq} i_{fg}} \quad (31)$$

For refrigerant the Nusselt No. correlation [27] during condensation in a vertical PHE given as

$$Nu_{r,tp,V} = Ge_5 \,\mathrm{Re}_{eq}^{Ge_6}\,\mathrm{Pr}^{0.33} \quad (32)$$

$$Ge_5 = 11.22\left(\frac{P_{co}}{D_h}\right)^{-0.2.83}\left(\frac{\pi}{2}-\beta\right)^{-4.5} \quad (33)$$

$$Ge_6 = 0.35\left(\frac{P_{co}}{D_h}\right)^{0.23}\left(\frac{\pi}{2}-\beta\right)^{1.48} \quad (34)$$

Hence corresponding convective heat transfer coefficients can be found out using basic eqn. 20.

Pressure drop in two-phase

In all four components combine together to give total pressure drop in two phase sections. These are pressure drop due to acceleration of the refrigerant, pressure drop due to elevation change because of height of PHE, pressure drop due to inlet and exit ports and most importantly pressure drop due to the friction inside the heat exchangers.

In evaporation the two phase friction factor is expressed as [26]

$$f_{tp,II} = Ge_3 \,\mathrm{Re}_{eq}^{Ge_4} \quad (35)$$

$$Ge_3 = 64710\left(\frac{P_{co}}{D_h}\right)^{-5.27}\left(\frac{\pi}{2}-\beta\right)^{-3.03} \quad (36)$$

$$Ge_4 = -1.314\left(\frac{P_{co}}{D_h}\right)^{-0.62}\left(\frac{\pi}{2}-\beta\right)^{-0.47} \quad (37)$$

In condensation the two-phase friction factor is given by [27]

$$f_{tp,V} = Ge_7 \,\mathrm{Re}_{eq}^{Ge_8} \quad (38)$$

$$Ge_7 = 3521.1\left(\frac{P_{co}}{D_h}\right)^{4.17}\left(\frac{\pi}{2}-\beta\right)^{-7.75} \quad (39)$$

$$Ge_8 = -1.024\left(\frac{P_{co}}{D_h}\right)^{0.0925}\left(\frac{\pi}{2}-\beta\right)^{-4.5} \quad (40)$$

In above all relations the constants from Ge_1 to Ge_8 are non-dimensional geometric parameters which rely upon certain plate heat exchanger geometrical parameters which are Hydraulic diameter (D_h), Corrugation pitch (P_{co}) and Chevron Angle (β) [26].

Frictional pressure drop is

$$\Delta P_f = \frac{4 f_{tp} N_{ch} G^2 L_e}{2\rho D_h} \quad (41)$$

The pressure drop due to acceleration is

$$\Delta P_{acc} = G_{eq}^2 x\left(v_g - v_f\right) \quad (42)$$

Here G_{eq} is the equivalent mass flux given by

$$G_{eq} = \frac{\dot{m}_{eq}}{b N_{ch} W_p} \quad (43)$$

The equivalent mass flow is defined as

$$\dot{m}_{eq} = \dot{m}\left[(1-x)+x\left(\frac{\rho_f}{\rho_g}\right)^{0.5}\right] \quad (44)$$

The change in pressure due to elevation positive upward is

$$\Delta P_{ele} = g \rho_m L_e \quad (45)$$

In above relation ρ_m is the mean density and is given

$$\frac{1}{\rho_m} = \left(\frac{x}{\rho_g} + \frac{1-x}{\rho_f}\right) \quad (46)$$

The port pressure drop for inlet and outlet manifolds is defined as

$$\Delta P_p = 1.4\frac{G_p^2}{\rho_m} \quad (47)$$

G_p is port mass flux given as

$$G_p = \frac{\dot{m}_{eq}}{\left(\frac{\pi D_p^2}{4}\right)} \quad (48)$$

The two-phase total pressure drop is as follows

$$\Delta P_{tp} = \Delta P_f + \Delta P_{acc} + \Delta P_{ele} + \Delta P_p \quad (49)$$

The overall pressure drop in evaporator PHE is

$$\Delta P_{evap} = \Delta P_{sf,I} + \Delta P_{tf,II} + \Delta P_{sf,III} \quad (50)$$

The overall pressure drop in vapor condenser PHE is

$$\Delta P_{cond} = \Delta P_{sf,IV} + \Delta P_{tf,V} \quad (51)$$

From one side heat transfer area of heat exchanger is obtained from LMTD method specified by eqns. 9 and 10 respectively and on the other side there is heat exchanger area value coming from the knowledge of initial selection of geometry of heat exchanger which is shown by eqn. 6. Iterative procedure is then put in action to find out the unique value of number of thermal plates, Np for which areas obtained from either side become identical in magnitude.

All fluid properties for heat source, working fluid and cooling source are calculated by taking average of the bulk temperatures at respective inlet and outlet state

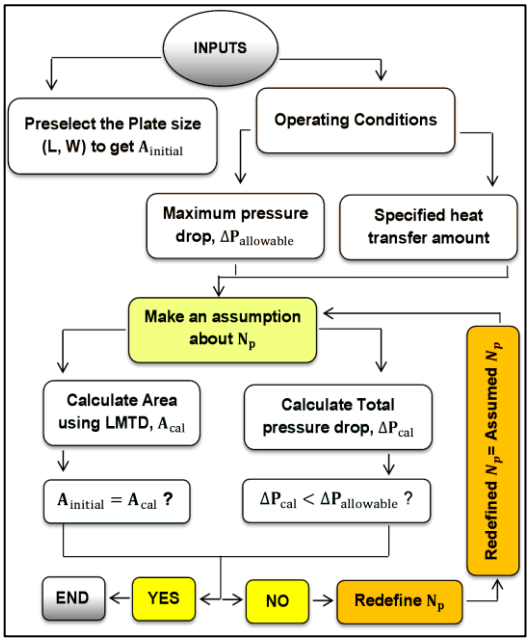

Fig. 4 Heat exchanger sizing layout

points [12].

7. ECONOMIC MODELLING OF SYSTEM

Economic modeling part of ORC system is discussed in this section. Chemical Engineering Plant Cost Index (CEPCI) of year 2013 has been implemented here in order to obtain the costs of all major components of the system. Atrens A. D. et al. [30] put up research for cost estimation regarding CO2 based EGS plant. The corresponding technique is utilized here to get the costs of all individual basic components of the system. The technique is also defined by [12, 31].

Cost of evaporator and condenser plate heat exchangers is found out by using one similar relation in which constants essentially depend upon the equipment (heat exchanger) type. In the current study we employed similar types of heat exchangers i.e. PHE so cost is given by

$$\mathrm{Cost}_{HX} = \frac{527.7}{397}\left(B_{1,HX} + B_{2,HX} F_{M,HX} F_{P,HX}\right) F_s C_{b,HX} \quad (52)$$

Here $B_{1,HX}$ and $B_{2,HX}$ are constants for particular type of heat exchanger. $F_{M,HX}$ is steel (SS) material factor. $F_{P,HX}$ is pressure factor of heat exchanger and is determined as

$$\log\left(F_{P,HX}\right) = C_{1,HX} + C_{2,HX}\log\left(P_{HX}\right) + C_{3,HX}\log\left(P_{HX}\right)^2 \quad (53)$$

Here $C_{1,HX}$, $C_{2,HX}$ and $C_{3,HX}$ are the constants based upon heat exchanger type. P_{HX} is design pressure of heat exchanger. In eqn. 52, F_s is the additional factor related to running and fixing costs for material, piping, labor and other extras. $C_{b,HX}$ is the basic cost whose calculation is governed by heat transfer area and a few constants as follows

$$\log\left(C_{b,HX}\right) = K_{1,HX} + K_{2,HX}\log\left(A_{HX}\right) + K_{3,HX}\left(\log\left(A_{HX}\right)\right)^2 \quad (54)$$

$K_{1,HX}$, $K_{2,HX}$ and $K_{3,HX}$ are the constants for heat exchanger type. A_{HX} is required area of heat exchanger (m^2).

Turbine is made up of SS and its cost is given by

$$\mathrm{Cost}_{TR} = \frac{527.7}{397}\left(F_{MP,TR} F_s C_{b,TR}\right) \quad (55)$$

$F_{MP,TR}$ is combine material and pressure factor for the turbine material of steel. F_s is already explained above. Basic cost of carbon steel turbine is as follows

$$\log(C_{b,TR}) = K_{1,TR} + K_{2,TR}\log(W_{TR}) + K_{3,TR}\left(\log(W_{TR})\right)^2 \quad (56)$$

Here $K_{1,TR}$, $K_{2,TR}$ and $K_{3,TR}$ are constants specifically for turbine. W_{TR} is turbine power output (kW). Centrifugal type of pump is used made of carbon steel material. Pump cost is expressed as

$$\mathrm{Cost}_{PP} = \frac{527.7}{397}\left(B_{1,PP} + B_{2,PP} F_{M,PP} F_{P,PP}\right) F_s C_{b,PP} \quad (57)$$

$B_{1,PP}$ and $B_{2,PP}$ are constants for type of pump which is centrifugal. $F_{M,PP}$ is the material factor and pressure factor $F_{P,PP}$ is given by

$$\log\left(F_{P,PP}\right) = C_{1,PP} + C_{2,PP}\log\left(P_{PP}\right) + C_{3,PP}\log\left(P_{PP}\right)^2 \quad (58)$$

$C_{1,PP}$, $C_{2,PP}$ and $C_{3,PP}$ are constants for centrifugal type of pump. P_{PP} is the design pressure (bars) for which pump is designed. In eqn. 57 F_s is the same factor as mentioned earlier for cost of heat exchangers. Basic cost of pump $C_{b,PP}$ is governed by the following relation

$$\log(C_{b,PP}) = K_{1,PP} + K_{2,PP}\log(W_{PP}) + K_{3,PP}\left(\log(W_{PP})\right)^2 \quad (59)$$

$K_{1,PP}$, $K_{2,PP}$ and $K_{3,PP}$ are constants for type of pump. W_{PP} denotes the power consumed by the pump (kW). The cost constants are enlisted in the Table 3 for heat exchangers, turbine and pump.

8. OBJECTIVE FUNCTIONS and NSGA-II

The two conflicting objective functions are expressed as

$$f_1(x) = \frac{\eta_{turb}\left(h_2 - h_3\right) - \dfrac{\left(h_1 - h_4\right)}{\eta_{pump}}}{\left(h_2 - h_1\right)} \quad (60)$$

$$f_2(x) = \frac{\eta_{turb}\left(h_2 - h_3\right) - \dfrac{\left(h_1 - h_4\right)}{\eta_{pump}}}{\left(\mathrm{Cost}_{HX,evap} + \mathrm{Cost}_{TR} + \mathrm{Cost}_{HX,cond} + \mathrm{Cost}_{PP}\right)} \quad (61)$$

Here $f_1(x)$ is the thermal efficiency function and is required to be maximized whereas $f_2(x)$ is SIC function and is deemed to be minimized by using NSGA-II. SIC is the ratio of net power output in kilo-watt of the system to its total cost in dollars. Negative sign is used with the thermal efficiency function in order to maximize it as the algorithm solves for evaluating minimum value. NSGA-II is a multi-objective optimization method and features a fast sorting and elitist preservation mechanism. Details can be found in literature [12, 13]. The parameters of NSGA-II were varied in the vicinity of their respectable range and results were compared with each other so that a set of parameters could be chosen to obtain healthy and best quality optimal results. Selection function is set as Tournament with a population size of 100, generations limit of 80, and 0.7 as crossover fraction. Uniform mutation function is chosen with 0.06 as mutation rate. Pareto front population fraction is 0.35.

Table 3 Cost constants for ORC system's misc components

Heat Exchangers		Turbine		Pump	
Con-stant	Value	Con-stant	Value	Con-stant	Value
F_s	1.70	F_s	1.70	F_s	1.70
$F_{M,HX}$	2.40	$F_{MP,TR}$	3.50	$F_{M,PP}$	2.20
$K_{1,HX}$	4.66	$K_{1,TR}$	2.2659	$K_{1,PP}$	3.3890
$K_{2,HX}$	-0.1557	$K_{2,TR}$	1.4398	$K_{2,PP}$	0.5360
$K_{3,HX}$	0.1547	$K_{3,TR}$	-0.1776	$K_{3,PP}$	0.1538
$B_{1,HX}$	0.96			$B_{1,PP}$	1.89
$B_{2,HX}$	1.21			$B_{2,PP}$	1.35
$C_{1,HX}$	0.00			$C_{1,PP}$	-0.3935
$C_{2,HX}$	0.00			$C_{2,PP}$	0.3957
$C_{3,HX}$	0.00			$C_{3,PP}$	-0.00226

8.1. Constraints selection for optimization

The constraints setting of decision variables for running optimization strictly depends upon each other along with important parameters such as heat source inlet temperature, critical temperature of working fluid and condensing temperature. For any working fluid the maximum saturation temperature in evaporator is always some amount lesser than heat source inlet temperature. For heat transfer to occur in right direction i.e. from heat source towards working fluid and working with subcritical cycle it has to be made sure that sum of evaporation temperature and PPTD across evaporator must be less than heat source inlet temperature and critical temperature of working fluid. Also sum of evaporation temperature and superheat at turbine inlet must be less than heat source inlet temperature. These criteria decide the upper bound for evaporation pressure. Whereas lower bound for evaporation pressure is controlled by condensing temperature. Previous investigations done by many researchers show only one set of upper and lower bounds of evaporation pressure for all organic compounds. And only one upper and lower bound means that it would have been selected by observing the minimum critical temperature out of all available refrigerants along with other parameters. But in this way the available potential of having higher upper limit present in other organic compounds is not fully utilized. Moreover waste heat resources are usually of low grade and demand precise use of available potential. In the current study each working fluids is given its own set of constraints for evaporation pressure by keeping its critical temperature, heat source temperature, maximum pinch point and superheat and condensing temperature in mind. With upper limit of superheat being 10 ℃ the evaporation pressure must be lesser than a pressure which has corresponding saturation temperature 10 ℃ less than heat source inlet temperature. Similarly with upper limit of evaporator pinch point being 25 ℃ the evaporation pressure must be lesser than a pressure which has corresponding saturation temperature 25 ℃ less than heat source inlet temperature. A minimum of 6 ℃ of pinch point necessitate effective heat transfer. Upper limit for pinch point across condenser depends upon cooling water inlet temperature and condensing temperature.

Having different evaporation pressure bounds for different fluids for same waste heat input conditions allows more search space availability for the genetic algorithm to look for an optimal solution of the problem. Table 4 summarizes the logical bounds of the decision variables set for multi-objective optimization.

Table 4 Logical bounds set for multiobjective optimization

Organic Fluid	P_e (kPa)	
	L.B[a]	U.B[b]
R-123	110	1320
R-1234ze	580	2200
R-152a	690	2775
R-21	215	2155
R-236ea	245	2105
R-245ca	122	1585
R-601	83	1000
Superheat (^{o}C)	0<Superheat<10	
$PPTD_{evap}$ (^{o}C)	6< $PPTD_{evap}$<25	
$PPTD_{cond}$ (^{o}C)	6< $PPTD_{cond}$<15	

([a]) Lower bound; ([b]) Upper bound

9. RESULTS AND DISCUSSION

Seven different refrigerants were used as working substances in the ORC system so as to decide which one is more compatible with the system under provided conditions than the rest based upon the dual objectives. For simulation heat source temperature is defined to be 150 ℃ having a mass flow rate of 7 kg/s. Cooling water is assumed to be entrying at 15 ℃ and condensing temperature is maintained at 30 ℃. The pareto-optimal fronts obtained from multi-objective optimization are shown in Figures 5 to 7 for refrigerants R-21, R-245ca and R-601 respectively. Table 5 summarizes all the results that show the objective function values and corresponding decision variables values. Actually pareto-optimal fronts define the solution lying in a range and best points selected are presented in Table 5.

It is clear that thermal efficiency varies from 8.59 % to 12.68 %. R-21 shows highest value of thermal efficiency while R-1234ze shows minimum thermal efficiency. R-123, R-601 and R-245ca give thermal efficiencies pretty close to that of R-21 with the difference being 0.31, 0.45 and 0.58 % respectively. R-152a is ahead of R-1234ze with thermal efficiency of 9.34 %.

The SIC varies between 6063.91 $/kW for R-245ca and 6465.64 $/kW for R-1234ze. Clearly R-245ca is found to be the most economical refrigerant whereas R-1234ze is the most uneconomical refrigerant among all considered refrigerants. So as far the thermal efficiency is concerned, R-21 is a suitable refrigerant and on the contrary, R-245ca finds its place as an appropriate refrigerant among all considered for giving low SIC. Results indicate that there is no single working fluid which provides highest thermal efficiency together with minimum SIC out of selected working fluids. One has to decide which objective function is more significant than the other in order to separate out the best working fluid. There is a trade-off situation between the two objectives. As far as waste heat resources are concerned, the important performance indicator is the net power output and researchers would like to maximize the power output rather than thermal efficiency and so minimize specific investment cost because it depends upon net power output. For R-245ca being most economical (6063$/kW) and for

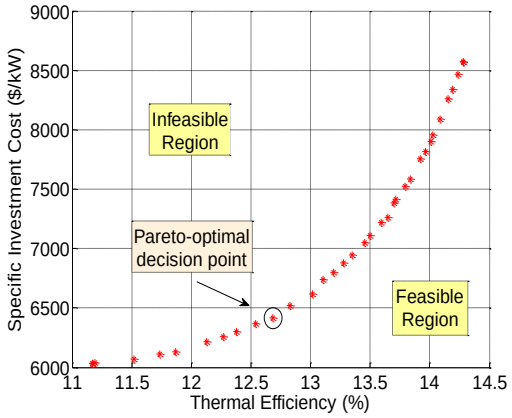

Fig. 5 Pareto-optimal front for R-21

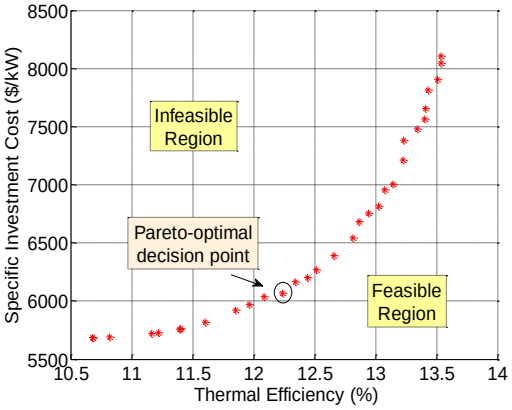

Fig. 6 Pareto-optimal front for R-245ca

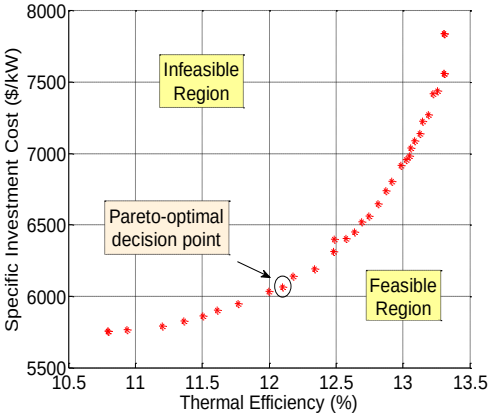

Fig. 7 Pareto-optimal front for R-601

analysis considering it to be basic refrigerant, merely a 0.14 % increment in thermal efficiency can be obtained at the expense of 7.92 $/kW by replacing R-601 as working fluid. 0.58 % of thermal efficiency can be increased by replacing R-21 at the expense of 354.33 $/kW which shows that this refrigerant is relatively more expensive and thus undesirable for the current system. It is better to use either R-245ca or R-601 as working fluids if SIC is required to be managed and R-21 should be used only if SIC is of little concern compared to thermal efficiency. R-123 depicts optimal solution closer to that of R-21 with SIC better optimized as compared to thermal efficiency. R-123 requires 44.21 $/kW less to give 0.31 % less efficiency compared to R-21. R-152a is economical, but less efficient

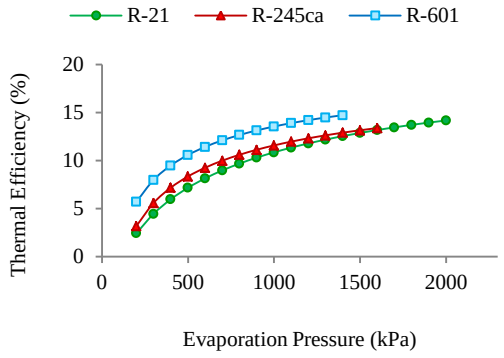

Fig. 8 Evaporation pressure vs thermal efficiency

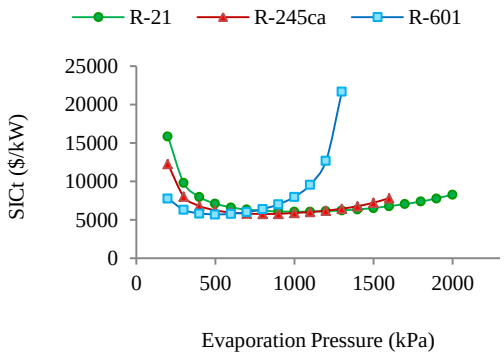

Fig. 9 Evaporation pressure vs SIC

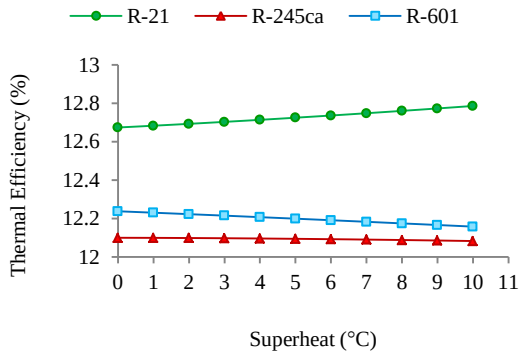

Fig. 10 Superheat vs thermal efficiency

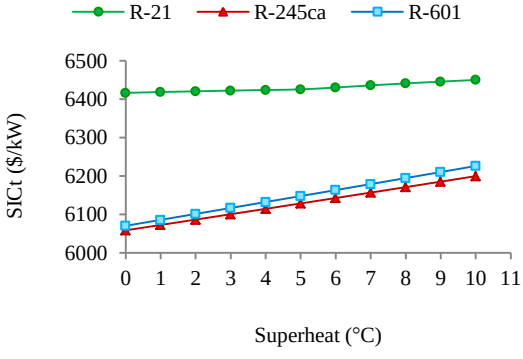

Fig. 11 Superheat vs SIC

thermodynamically. See Table 5 for all values. Moreover out of these refrigerants R-601 has the best performance checked out by taking the ratio of values of the two objective functions i.e. the ratio of SIC and thermal efficiency and that is minimum for R-601. This can be another indicator for decision making.

Four decision variables had been selected based upon their attribute of having strong influence on the two objective

functions. Detailed sensitivity analysis was carried out for R-21, R-245ca and R-601 because of their best thermal efficiency, lowest SIC and minimal value of the ratio of SIC and thermal efficiency respectively. While one parameter was varied others were kept constant at their respective optimal solution values. Thermal efficiency and SIC strictly depend upon how the contributing parameters relatively change.

Fig. 8 shows that increase in evaporation pressure results in increase in the thermal efficiency governed by two parameters i.e. net power output and heat supplied in evaporator. There is found one typical value of evaporation pressure which decides how the two governing parameters are going to behave. Later on after passing the typical value of evaporation pressure the net power output starts decreasing but overall thermal efficiency keeps on increasing subjected to fast increase in net power output and slow increase in total cost. Beyond the point enhancement of evaporation pressure leads the total cost to decrease at a higher rate than the net power output hence SIC increases as shown in Fig. 9. As far as the trend and pattern is concerned the result is in accordance with research done by Imran M. et al. [10].

The superheating control before vapor go into turbine inlet does not exert persuasive influence over thermal efficiency. Results conclude that thermal efficiency is affected only by 0.95 % increase when superheat is raised from 0 to 10 ℃ for R-21. Corresponding change for R-245ca and R-601 is 0.14 % and 0.65 % decrease. R-21 being wet fluid gets

Table 5 Pareto-optimal solution obtained after multiobjective optimization

Refrigerant	Twin objectives		Decision variables			
	η_{th} %	SIC $/kW	P_{evap} kPa	Superheat °C	$PPTD_{evap}$ °C	$PPTD_{cond}$ °C
R-123	12.37	6374.03	934.84	0.53	6.59	14.61
R-1234ze	8.59	6465.64	2187.47	0.99	12.74	14.80
R-152a	9.34	6086.97	2765.03	0.96	8.95	14.82
R-21	12.68	6418.24	1541.93	0.94	6.50	14.64
R-236ea	11.42	6068.80	2003.69	0.17	6.83	14.85
R-245ca	12.10	6063.91	1136.71	0.39	7.05	14.89
R-601	12.24	6071.83	722.37	0.11	7.04	14.59

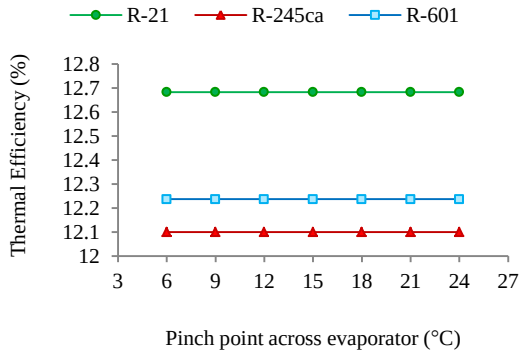

Fig. 12 Evaporator pinch point vs thermal efficiency

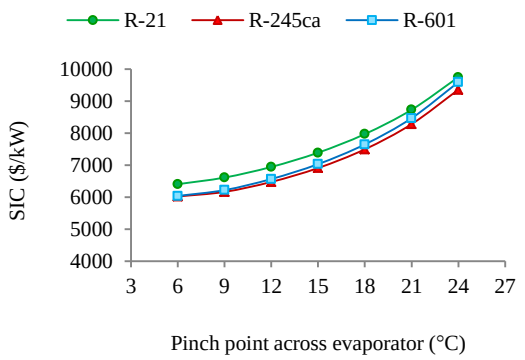

Fig. 13 Evaporator pinch point vs SIC

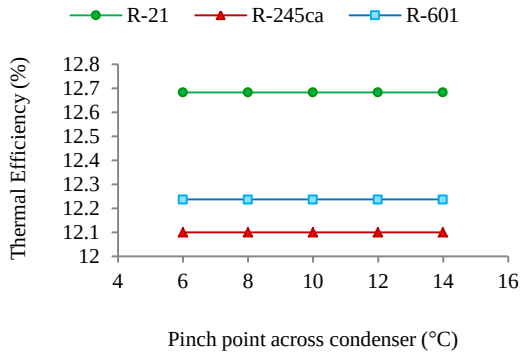

Fig. 14 Condenser pinch point vs thermal efficiency

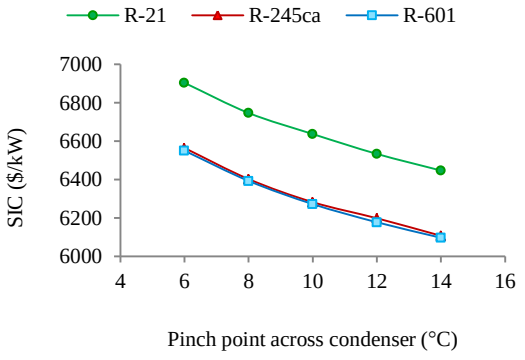

Fig. 15 Condenser pinch point vs SIC

increase in thermal efficiency while converse behavior is exhibited by dry fluids R-245ca and R-601. Increase in superheat decreases the net power output as well as heat gained by working fluid in the evaporator for all refrigerants. For R-21 reduction of net power output dominates the heat gained reduction giving positive slope of curve while for R-245ca and R-601 net power output fall is dominated by heat reduction in evaporator resulting in negative slope of the curves as given in Fig. 10. Fig. 11 demonstrates that

superheating at turbine inlet has direct influence over SIC. Superheating decreases the area of evaporator demanded by lesser amount of heat transfer thus decreasing the total cost which surpasses the fall in net power output eventually yielding an increase in SIC.

Thermal efficiency is not affected by the pinch point temperature difference across evaporator and condenser

under the operating conditions set for investigating the ORC system. This is because PPTD across evaporator and condenser heat exchangers was set to be independently determining the heat source side and cooling water side temperatures respectively. Furthermore refrigerant mass flow rate gets decreased (heat source flow rate is independently fixed) after increasing the PPTD across evaporator causing reduction in net power output and heat transfer in evaporator in equal proportion (Fig. 12). Changing PPTD across condenser has no effect on either parameter deciding thermal efficiency (Fig. 14).

PPTD across evaporator needs to be lesser for economical design of ORC system. Higher the PPTD across evaporator lower is the net power output because of lower mass flow rate of refrigerant required. Total cost of ORC system also decreases as a result of reduced turbine and pump work and area required for heat transfer to take place. The decrease of net power output is dominant that leads to increase SIC (Fig. 13). Larger PPTD across condenser tends to decrease the SIC (Fig. 15).

10. CONCLUSIONS

Seven refrigerants were given opportunity to show the thermo-economic behavior of an ORC system having a geothermal source at its background. The key features of the research include creation of numerical simulation model on MATLAB and use of multi-objective optimization method NSGA-II for obtaining optimal solution of set objectives.

It is found that no refrigerant is best at the same time for fulfilling two conflicting objectives. R-21 gives highest thermal efficiency value while R-245ca is the most economical. R-601 is better than R-21 as it loses 0.446 % of efficiency but gains 346.41 $/kW benefit.

- Out of all decision variables evaporation pressure significantly affect the objective functions. Each working medium has its own range of evaporation pressure where it gives highest thermal efficiency together with lowest SIC.Superheat optimal value is close to its lower boundary value (less than 1℃) and it is verified from Figures 10 and 11 that thermal efficiency is not effectively increased rather there is increase in SIC as a whole if superheat is raised.
- The optimal pinch point is located at upper boundary for condenser and lower boundary for evaporator. The pinch point temperature difference across any heat exchanger does not affect thermal efficiency of the system at all.

NOMENCLATURE

A	heat exchanger area (m^2)
A_f	channel flow area (m^2)
A_{1p}	projected area per plate (m^2)
A_p	developed area per plate (m^2)
b	mean channel spacing (m)
Bo	Boiling number
Cp	specific heat capacity ($J/kg.K$)
D	diameter (m)
f	friction factor
G	mass flux ($kg/s.m^2$)
GA	Genetic Algorithm
GWP	Global Warming Potential
h	enthalpy (kJ/s)
HPCD	horizontal port center distance (m)
k	thermal conductivity ($W/m.K$)
L	length of plate (m)
LMTD	Log Mean Temperature Difference (℃)
$\dot{m}$	mass flow rate (kg/s)
Np	number of thermal plates
Nu	Nusselt number
ODP	Ozone Depletion Potential
p	plate pitch (m)
PHE	plate heat exchanger
PPTD	Pinch Point Temperature Difference (℃)
Pr	Prandtl numeber
Q	rate of heat transfer (kW)
$\ddot{q}$	average imposed heat flux (W/m^2)
Re	Reynolds number
SIC	specific investment cost ($/kW)
t	plate thickness (m)
U	overall heat transfer coefficient ($W/m^2.K$)
VPCD	vertical port center distance (m)
W	rate of work (kW), width of plate (m)
WHR	waste heat recovery
ΔP	pressure drop (kPa)

Greek letters

α	convective heat transfer coefficient ($W/m^2.K$)
β	chevron angle (deg)
ϕ	enlargement factor
η	thermal efficiency (%)
λ	corrugation pitch (m); P_{co}
μ	viscosity (Pa.s)
ρ	density (kg/m^3)

Subscripts

acc	acceleration
ch	channel
cond	condenser
e	equivalent, effective
ele	elevation
evap	evaporator
f,g	saturated liquid and vapors state
h	hydraulic
m	mean
p	plate, port
r	refrigerant side
sp	single phase
tp	two phase
turb	turbine
w	water side
I	preheating stage
II	evaporation stage
III	superheating stage
IV	desuperheating stage
V	condensing stage

REFRENCES

1. Yamamoto, T., et al., Design and testing of the organic Rankine cycle. *Energy*, 2001. **26**(3): p. 239-251.
2. Desai, N.B. and S. Bandyopadhyay, Process integration of organic Rankine cycle. *Energy*, 2009. **34**(10): p. 1674-1686.
3. Tchanche, B.F., et al., Low-grade heat conversion into power using organic Rankine cycles–a review of various applications. *Renewable and Sustainable Energy Reviews*, 2011. **15**(8): p. 3963-3979.
4. Bao, J. and L. Zhao, A review of working fluid and expander selections for organic Rankine cycle. *Renewable and Sustainable Energy Reviews*, 2013. **24**: p. 325-342.
5. Hung, T.-C., Waste heat recovery of organic Rankine cycle using dry fluids. *Energy Conversion and Management*, 2001. **42**(5): p. 539-553.
6. Stijepovic, M.Z., et al., On the role of working fluid properties in Organic Rankine Cycle performance. *Applied Thermal Engineering*, 2012. **36**: p. 406-413.

7. Chen, H., D.Y. Goswami, and E.K. Stefanakos, A review of thermodynamic cycles and working fluids for the conversion of low-grade heat. *Renewable and sustainable energy reviews*, 2010. **14**(9): p. 3059-3067.
8. Quoilin, S., et al., Thermo-economic optimization of waste heat recovery Organic Rankine Cycles. *Applied Thermal Engineering*, 2011. **31**(14): p. 2885-2893.
9. Quoilin, S. and V. Lemort. Technological and economical survey of organic Rankine cycle systems. *in European conference on Economics and management of energy in industry*. 2009.
10. Imran, M., et al., Thermo-economic optimization of Regenerative Organic Rankine Cycle for waste heat recovery applications. *Energy Conversion and Management*, 2014. **87**: p. 107-118.
11. Imran, M., et al., Multi-objective optimization of evaporator of organic Rankine cycle (ORC) for low temperature geothermal heat source. *Applied Thermal Engineering*, 2015. **80**: p. 1-9.
12. Wang, J., et al., Multi-objective optimization of an organic Rankine cycle (ORC) for low grade waste heat recovery using evolutionary algorithm. *Energy Conversion and Management*, 2013. **71**: p. 146-158.
13. Wang, J., et al., Thermodynamic analysis and optimization of an (organic Rankine cycle) ORC using low grade heat source. *Energy*, 2013. **49**: p. 356-365.
14. Wang, J., et al., Multi-objective optimization design of condenser in an organic Rankine cycle for low grade waste heat recovery using evolutionary algorithm. *International Communications in Heat and Mass Transfer*, 2013. **45**: p. 47-54.
15. Carcasci, C., R. Ferraro, and E. Miliotti, Thermodynamic analysis of an organic Rankine cycle for waste heat recovery from gas turbines. *Energy*, 2014. **65**: p. 91-100.
16. Rettig, A., et al. Application of organic Rankine cycles (ORC). *in Proceedings of the World Engineer's Convention, Geneva, Switzerland*. 2011.
17. Bruno, J.C., et al., Modelling and optimisation of solar organic rankine cycle engines for reverse osmosis desalination. *Applied Thermal Engineering*, 2008. **28**(17): p. 2212-2226.
18. Roy, J. and A. Misra, Parametric optimization and performance analysis of a regenerative Organic Rankine Cycle using R-123 for waste heat recovery. *Energy*, 2012. **39**(1): p. 227-235.
19. Maraver, D., et al., Systematic optimization of subcritical and transcritical organic Rankine cycles (ORCs) constrained by technical parameters in multiple applications. *Applied energy*, 2014. **117**: p. 11-29.
20. Quoilin, S., et al., Techno-economic survey of Organic Rankine Cycle (ORC) systems. *Renewable and Sustainable Energy Reviews*, 2013. **22**: p. 168-186.
21. Wang, D., X. Ling, and H. Peng, Performance analysis of double organic Rankine cycle for discontinuous low temperature waste heat recovery. *Applied Thermal Engineering*, 2012. **48**: p. 63-71.
22. Xi, H., et al., Parametric optimization of regenerative organic Rankine cycle (ORC) for low grade waste heat recovery using genetic algorithm. *Energy*, 2013. **58**: p. 473-482.
23. García-Cascales, J., et al., Assessment of boiling and condensation heat transfer correlations in the modelling of plate heat exchangers. *International Journal of Refrigeration*, 2007. **30**(6): p. 1029-1041.
24. Ayub, Z.H., Plate heat exchanger literature survey and new heat transfer and pressure drop correlations for refrigerant evaporators. *Heat Transfer Engineering*, 2003. **24**(5): p. 3-16.
25. Hsieh, Y. and T. Lin, Saturated flow boiling heat transfer and pressure drop of refrigerant R-410A in a vertical plate heat exchanger. *International Journal of Heat and Mass Transfer*, 2002. **45**(5): p. 1033-1044.
26. Han, D.-H., K.-J. Lee, and Y.-H. Kim, Experiments on the characteristics of evaporation of R410A in brazed plate heat exchangers with different geometric configurations. *Applied thermal engineering*, 2003. **23**(10): p. 1209-1225.
27. Han, D.-H., K.-J. Lee, and Y.-H. Kim, The characteristics of condensation in brazed plate heat exchangers with different chevron angles. *JOURNAL-KOREAN PHYSICAL SOCIETY*, 2003. **43**: p. 66-73.
28. Walraven, D., B. Laenen, and W. D'haeseleer, Comparison of shell-and-tube with plate heat exchangers for the use in low-temperature organic Rankine cycles. *Energy Conversion and Management*, 2014. **87**: p. 227-237.
29. Jung, H. and S. Krumdieck, Modelling of organic Rankine cycle system and heat exchanger components. International Journal of Sustainable Energy, 2014. 33(3): p. 704-721.
30. Atrens, A.D., H. Gurgenci, and V. Rudolph, Economic optimization of a CO2-based EGS power plant. *Energy & Fuels*, 2011. **25**(8): p. 3765-3775.
31. Li, M., et al., Thermo-economic analysis and comparison of a CO 2 transcritical power cycle and an organic Rankine cycle. *Geothermics*, 2014. **50**: p. 101-111.
32. NIST Standard Reference Database 23. *NIST Thermodynamic and Transport Properties of Refrigerants and Refrigerant Mixtures REFROP*, Version 9.0, 2010